PHYSICAL REVIEW APPLIED **6,** 041001 (2016)

Origin and Reduction of $1/f$ Magnetic Flux Noise in Superconducting Devices

P. Kumar,[1] S. Sendelbach,[1,*] M. A. Beck,[1] J. W. Freeland,[2] Zhe Wang,[3,4] Hui Wang,[3,4] Clare C. Yu,[3] R. Q. Wu,[3] D. P. Pappas,[5] and R. McDermott[1,†]

[1]*Department of Physics, University of Wisconsin–Madison, Madison, Wisconsin 53706, USA*
[2]*Advanced Photon Source, Argonne National Laboratory, Argonne, Illinois 60439, USA*
[3]*Department of Physics and Astronomy, University of California, Irvine, California 92617, USA*
[4]*State Key Laboratory of Surface Physics and Key Laboratory for Computational Physical Sciences, Fudan University, Shanghai 200433, China*
[5]*National Institute of Standards and Technology, Boulder, Colorado 80305, USA*

(Received 5 April 2016; revised manuscript received 24 August 2016; published 18 October 2016)

Magnetic flux noise is a dominant source of dephasing and energy relaxation in superconducting qubits. The noise power spectral density varies with frequency as $1/f^{\alpha}$, with $\alpha \lesssim 1$, and spans 13 orders of magnitude. Recent work indicates that the noise is from unpaired magnetic defects on the surfaces of the superconducting devices. Here, we demonstrate that adsorbed molecular O_2 is the dominant contributor to magnetism in superconducting thin films. We show that this magnetism can be reduced by appropriate surface treatment or improvement in the sample vacuum environment. We observe a suppression of static spin susceptibility by more than an order of magnitude and a suppression of $1/f$ magnetic flux noise power spectral density of up to a factor of 5. These advances open the door to the realization of superconducting qubits with improved quantum coherence.

DOI: 10.1103/PhysRevApplied.6.041001

Low-frequency $1/f$ magnetic flux noise was first identified in the 1980s when superconducting quantum interference device (SQUID) circuits were cooled to millikelvin temperatures in an effort to reach quantum-limited sensitivity for applications such as gravity-wave detection [1]. While the white noise level of these devices decreases as expected with decreasing temperature, an excess low-frequency flux noise persists to the lowest temperatures. The flux noise power spectral density scales with frequency as $1/f^{\alpha}$ with $\alpha \lesssim 1$; interestingly, the magnitude of this excess noise is roughly independent of device scale and materials [1]. At the time, many noise sources were ruled out; however, the microscopic origin of the noise was never identified. The source of flux noise has remained a longstanding puzzle in condensed matter physics [2].

More recently, it has been realized that this noise is a dominant source of dephasing in superconducting quantum bits ("qubits") [3–5], a leading candidate for scalable quantum information processing in the solid state [6–8]. In the context of a quantum annealer [9,10], flux noise degrades performance by limiting the number of qubits that can tunnel coherently. For these reasons, there is strong motivation to understand and eliminate the flux noise.

Recent experiments indicate that there is a high density of unpaired surface spins in superconducting integrated circuits [11], and it is now believed that fluctuations of these spins give rise to the $1/f$ flux noise [12–14]. There is experimental evidence that interactions between the surface spins are significant [15]. To date, however, there has been no experimental data pointing toward the microscopic nature of the surface magnetic defects, although there has been speculation that the defects are due to localized states at the disordered metal-insulator interface [16] or to surface adsorbates [17], molecular O_2 in particular [13].

Here, we describe x-ray absorption spectroscopy (XAS) and x-ray magnetic circular dichroism (XMCD) experiments that point to adsorbed molecular O_2 as the dominant source of surface magnetism in superconducting thin films. We show that improvement of the vacuum environment of the superconducting sample and appropriate surface passivation can dramatically reduce the surface density of spins in superconducting thin films. We present data on the surface spin susceptibility and magnetic flux noise of devices before and after various surface treatments and demonstrate a significant suppression of magnetic activity and flux noise power. Our results rule out prevailing theoretical models that invoke localized defects at the metal-insulator interface [16] that interact via the Ruderman-Kittel-Kasuya-Yosida mechanism [12]. Moreover, the implication of an extrinsic noise source provides a natural explanation for the observed weak dependence of the noise on device materials [1]. The achieved noise reduction opens the door to development of improved qubits with extended coherence times.

Using the Advanced Photon Source at Argonne National Laboratory, we perform XAS and XMCD experiments on

*Present address: Northrop Grumman Corporation, Linthicum, Maryland 21203, USA.
†rfmcdermott@wisc.edu

aluminum and niobium thin-film samples. In XMCD, one monitors the absorption of a spin-polarized sample at specific x-ray edges; the x-ray energy provides elemental specificity, while the x-ray helicity provides access to orbital magnetism. Devices are cooled to 10 K, and XMCD experiments are performed in fields of up to 5 T. Initially, we examine sputtered Al and Nb films cooled in ultrahigh vacuum (UHV; $P \lesssim 10^{-9}$ Torr); we expect these films to be covered by an amorphous native oxide due to prolonged exposure to atmosphere. We examine the Al and O K edges in the Al films and the Nb L edge and the O K edge in the Nb films and observe no XMCD signal at any of these energies [Fig. 1(a), upper trace]. However, when we intentionally degrade the vacuum of the sample

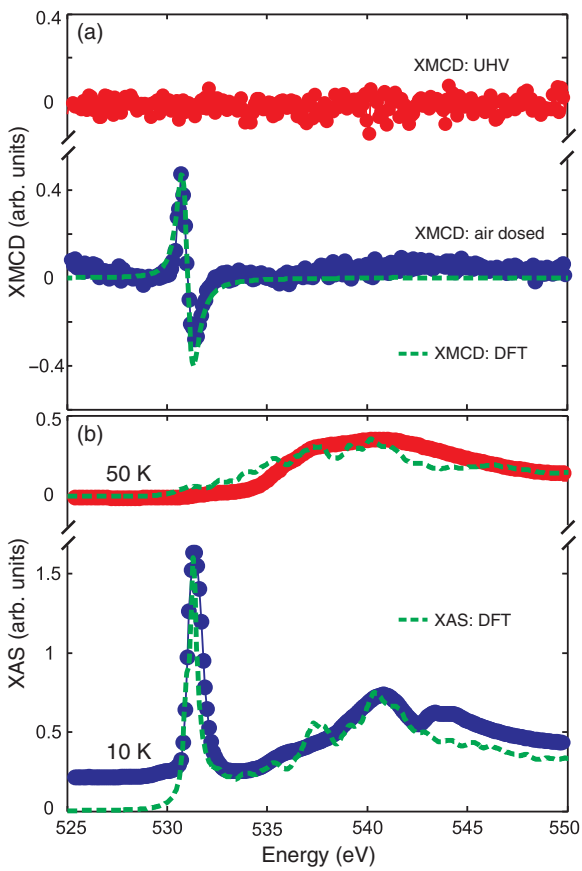

FIG. 1. (a) X-ray magnetic circular dichroism (XMCD) at the oxygen K edge for a native Al film and an Al film exposed to air. The native film (top) shows no XMCD signal, while the air-exposed film (bottom) shows a clear XMCD signal at 531 eV. (Traces are offset for clarity.) A similar XMCD signal at the oxygen K edge is seen for Nb films exposed to air (not shown). (b) Oxygen K-edge x-ray absorption spectroscopy (XAS) of an Al thin film cooled in the presence of 5×10^{-8} Torr O_2. Beginning at around 45 K, we observe a sharp peak at 531 eV and a broad spectral feature from 535–550 eV which we ascribe to adsorbed molecular O_2. (Traces are offset for clarity.) Dashed lines are from DFT simulations for Al_2O_3 (XAS at 50 K) and for O_2/Al_2O_3 (XMCD and XAS at 10 K); see the Supplemental Material [18] for details.

cryostat by bleeding in air or dry O_2 gas at a pressure on the order of 10^{-6} Torr for several minutes, we observe a clear XMCD signal at the O K edge [Fig. 1(a), lower trace]. Density-functional-theory (DFT) modeling allows us to assign the measured XMCD signal to molecular O_2 [dashed line in Fig. 1(a)]. In a separate series of experiments, we expose the metal thin film continuously to oxygen as we cool down from room temperature in an O_2 partial pressure of 5×10^{-8} Torr; the experimental data and the corresponding DFT calculations are shown in Fig. 1(b). We observe a strong modification of the O K-edge XAS signal starting at a temperature of around 45 K, indicating the onset of significant adsorption. By comparing the spectral weight of the broad feature from 535–550 eV in the high-temperature spectra to that of the narrow peak at 531 eV in the low-temperature spectra, we can roughly quantify the amount of adsorbed oxygen relative to that bound in the native oxide of the metal. We conclude that the films are covered by one to two monolayers of adsorbed O_2. The best agreement between DFT and the measured XMCD and XAS signals occurs when the O_2 bond is tilted with respect to the beam direction. This result is consistent with prior DFT calculations of O_2 adsorbed on Al_2O_3 (0001), which indicate that the molecular bond axis is tilted 55° from the surface normal [13].

The XMCD results suggest that the dominant magnetism in Al and Nb thin films of the type used to make qubit circuits is due not to a high density of intrinsic defects, but rather to adsorbed molecular O_2. The outermost electrons of the O_2 molecule form a spin-1 triplet state [13]. O_2 is paramagnetic at high temperatures; at low temperatures, solid molecular O_2 displays a complex phase diagram with multiple competing magnetic orders [19]. In typical superconducting qubit experiments, devices are cooled to millikelvin temperatures in vacuum cryostats that achieve pressures on the order of 10^{-6} Torr prior to cooldown; this pressure corresponds to an adsorption rate of roughly 1 ML/s, assuming a unit sticking coefficient. Even when the cryostat is cold, there is a continual flux of molecules from hot regions of the cryostat to the cold regions where the sample is housed. Thus, an accumulation of magnetic O_2 on the surface of these devices is inevitable.

This realization motivates us to attempt noise reduction by improving the vacuum environment of the superconducting devices. To this end, we have designed a hermetic sample enclosure based on grade 5 titanium alloy (Ti-6Al-4V); see the Supplemental Material [18]. In Fig. 2 we show the details of the enclosure and the sample prep chamber. The sample box is pumped through a copper pinch tube with a turbomolecular pump and an ion pump. During evacuation, the sample enclosure and chamber are baked to 120 °C. Following vacuum bake, the sample cell is cooled to room temperature and the cell is hermetically sealed using a commercial pinch tool. In some cases, the sample cell is backfilled with NH_3 gas prior to pinch-off. In other

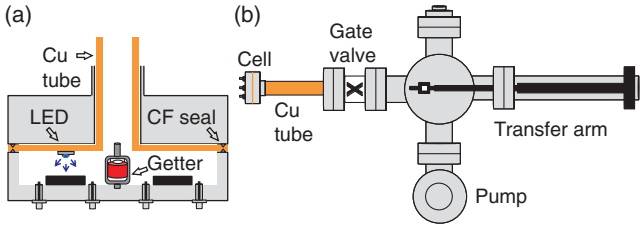

FIG. 2. (a) Schematic of hermetic grade 5 titanium enclosure for susceptibility and flux noise measurements. The enclosure incorporates weld-in SMA feedthroughs and a single 2.75″ ConFlat gasket. (b) Schematic of the sample prep chamber. The chamber incorporates a turbo pump, an ion pump, and a transfer arm used to install the NEG in the sample cell.

cases, the sample is irradiated with UV light (365 nm) during evacuation to promote photodesorption of strongly bound magnetic species, and a nonevaporable getter (NEG) pill (SAES, Inc.) is activated in a separate chamber and transferred into the sample enclosure under vacuum. The NEG provides continuous pumping in the sample cell following pinch-off.

In the first series of experiments, we characterize the surface spin density on washer-style Nb SQUIDs by monitoring the temperature-dependent zero-frequency surface spin susceptibility of field-cooled devices [11]. The device layout is shown in the inset of Fig. 3. Here, we intentionally trap flux vortices in the thin films of the Nb SQUID by cooling through the superconducting transition in the presence of an applied magnetic field. Any unpaired magnetic defects on the surface of the device develop a thermal polarization in the relatively strong (tens of mT) local fields in the vortex core. As temperature decreases, the thermal polarization of the defect spins increases. The flux through the SQUID loop thus displays a roughly $1/T$ Curie-like dependence on temperature, and the measured flux change can be used to extract a surface density of unpaired spins. For typical devices, we infer a surface spin density on the order of 10^{17} m^{-2} [11,20].

In Fig. 3 we compare baseline data to data from a cell that is evacuated and then backfilled with NH_3 gas at approximately 100 Torr prior to pinch-off. The temperature-dependent flux is suppressed by roughly an order of magnitude. Nonmagnetic NH_3 has a higher free energy of adsorption than O_2 (1.5 versus 0.15 eV according to our DFT calculations on Al_2O_3). Hence, it occupies available surface sites that would otherwise be taken up by magnetic O_2, resulting in a suppression of the surface density of adsorbed spins; related approaches to suppressing magnetic adsorbates were suggested in Refs. [13,17].

Both susceptibility and magnetization noise scale linearly with spin density, and reduction in the density of surface spins should yield a reduction in flux noise power. In the final series of experiments, we have examined the flux noise of Al-based SQUIDs subjected to various surface treatments; the results are presented in Fig. 4 and Table I. In

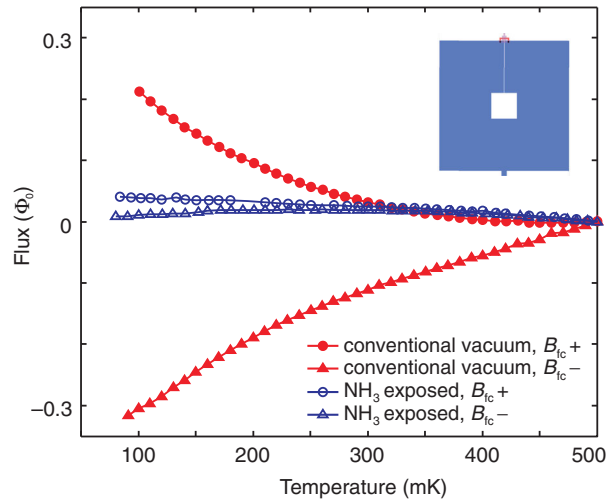

FIG. 3. Temperature-dependent flux threading a square-washer Nb SQUID (350 pH; see inset) cooled in a conventional vacuum (closed red symbols) and cooled following vacuum bake and NH_3 passivation (open blue symbols). The upper (lower) branches correspond to cooling fields of $+128$ μT (-128 μT). The magnitude of the flux change is proportional to the density of magnetically active surface spins [11].

these experiments, the Al-based first-stage device under test (DUT) is biased with a voltage, and the fluctuating current through the DUT is measured with a second Nb-based SQUID; measurements are performed in an adiabatic demagnetization refrigerator at a temperature of 100 mK. We characterize devices where the SQUID loop is encapsulated either in SiN_x or SiO_x grown by plasma-enhanced chemical vapor deposition. The SQUIDs described here are designed with a relatively high loop aspect ratio (ratio of loop width to trace width) of 25, as this geometry enhances the coupling of surface spin fluctuations to the device [5,14,21] (see the Supplemental Material [18]). We fit the measured noise spectra to the form $A/f^{\alpha} + B$, and we compare the $1/f$ noise power A and noise exponent α measured on identical devices before and after surface treatment.

In the case of SQUIDs encapsulated in SiN_x, we observe a significant noise reduction for both devices passivated with NH_3 and devices cooled in an improved vacuum following UV illumination. Figure 4(a) shows before and after spectra from one sample that was baked in the titanium cell and passivated with NH_3 using the protocol described above. The flux noise power spectral density at 1 Hz decreases from 8.2 to 1.6 $\mu\Phi_0^2$/Hz. In Fig. 4(b) we show before and after spectra from a device that was subjected to UV illumination and cooled in an improved vacuum; here, the flux noise power spectral density at 1 Hz decreases from 1.7 to 0.35 $\mu\Phi_0^2$/Hz. We examine a total of six SiN_x-encapsulated devices; the results are summarized in the table. For these devices, we observe a magnetic flux noise level of 3.9 ± 2.2 $\mu\Phi_0^2$/Hz at 1 Hz prior to

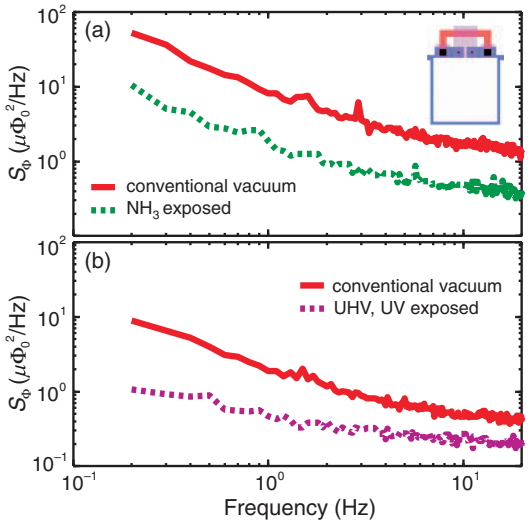

FIG. 4. (a) Flux noise spectra of SQUID device $SiN_x - 4$ before (upper trace) and after (lower trace) vacuum bakeout and NH_3 passivation. (Inset) Device layout. (b) Flux noise spectra of SQUID device $SiN_x - 6$ before (upper trace) and after (lower trace) vacuum bakeout and UV illumination.

surface treatment, with the noise exponent $\alpha = 0.95 \pm 0.17$. Following treatment, we find a noise level $1.7 \pm 1.0\ \mu\Phi_0^2/\ \mathrm{Hz}$ at 1 Hz with the noise exponent $\alpha = 0.83 \pm 0.18$. A noise reduction is seen in every SiN_x-encapsulated device, with an average reduction in S_Φ (1 Hz) by a factor of 2.8 and a maximum noise reduction by a factor of 5.1. We remark that repeated noise measurements on individual devices (even following thermal cycle to 300 K) show very little variation in the absence of surface modification (see the Supplemental Material [18]); the robustness of the noise spectrum to thermal cycling suggests that fixed disorder at the surface dictates how the O_2 molecules are adsorbed or, alternatively, that strongly bound magnetic species persist to high temperatures, providing a noise "fingerprint". To our knowledge, the $1/f$ flux noise measured in our surface-treated nitride devices is the lowest reported in the literature, when the noise is appropriately scaled by device aspect ratio.

TABLE I. Noise reduction by vacuum and surface treatment. The table includes results of before and after measurements on six SQUIDs with SiN_x loop encapsulation ($SiN_x - 1, \ldots, 6$) and four SQUIDs with SiO_x loop encapsulation ($SiO_x - 1, \ldots, 4$). Relative uncertainties in flux noise power spectral density S_Φ (1 Hz) and noise exponent α are 10% and 25%, respectively, as determined from repeated measurements following thermal cycling (see the Supplemental Material [18]).

	Pretreatment			Post-treatment	
Device	S_Φ (1 Hz) ($\mu\Phi_0^2$/Hz)	α	Treatment	S_Φ (1 Hz) ($\mu\Phi_0^2$/Hz)	α
$SiN_x - 1$	2.0	1.0	UHV	1.4	1.1
$SiN_x - 2$	4.4	0.7	NH_3	2.4	0.7
$SiN_x - 3$	2.8	1.0	UHV, UV	1.3	0.9
$SiN_x - 4$	8.2	1.2	NH_3	1.6	1.1
			UHV, UV	4.2	0.8
$SiN_x - 5$	4.1	0.8	NH_3	1.7	0.7
			UHV, UV	1.1	0.6
$SiN_x - 6$	1.7	1.0	NH_3	1.1	0.9
			UHV, UV	0.35	0.6
$SiO_x - 1$	13.4	0.5	UHV, UV	13.7	0.5
$SiO_x - 2$	6.5	1.0	UHV, UV	2.5	0.9
$SiO_x - 3$	4.8	0.7	UHV, UV	5.1	1.1
$SiO_x - 4$	3.0	0.8	UHV, UV	5.4	0.8

In the case of SiO_x-encapsulated devices subjected to UV irradiation under vacuum, no clear noise suppression is seen. We speculate that the UV photon energy of 3.4 eV is large enough to break bonds in the encapsulating oxide, perhaps liberating additional oxygen and providing another path for magnetic contamination.

Our ability to reduce $1/f$ flux noise power by up to a factor of 5 indicates clearly that adsorbates are the dominant source of low-frequency flux noise in our devices. It is reasonable to ask why the noise reduction is not larger. It could be that the remaining noise is still dominated by residual adsorbates. We measure pressure in the 10^{-9} Torr range at the ion pump, and pressure in the cell is likely an order of magnitude higher. Improvements in vacuum could lead to further noise reduction. Once again, the suppression of static spin susceptibility in the Nb SQUID described in Fig. 3 is larger than the noise reductions in Al-based devices described in Fig. 4 and Table I. This discrepancy suggests that the details of the disordered surface play a critical role in dictating the adsorption and/or fluctuation dynamics of the O_2 moments. We do measure systematically higher flux noise in oxide-encapsulated devices, and we have seen an increase in the flux noise of the nitride-encapsulated devices over the course of several years prior to this investigation of surface treatments, presumably due to uncontrolled evolution of the disordered surface; see the Supplemental Material [18]. Alternatively, it could be that the residual noise is due to some other magnetic states that are immune to the surface treatments described here.

Our DFT calculations indicate that an O_2 molecule adsorbed on Al_2O_3 (0001) sits atop Al atoms and has a moment of $1.8\mu_B$ that rotates almost freely in the plane perpendicular to the molecular axis (with a barrier to spin rotation of approximately 10 mK) [13,22–24]. $1/f$ noise results from a distribution of relaxation times [25] that can arise from interactions. DFT finds that neighboring O_2 molecules on Al_2O_3 have ferromagnetic exchange, and Monte Carlo simulations show that a distribution of ferromagnetic interactions produces $1/f$ noise consistent with experiment [13]. Surface disorder could change the magnitude and sign of these interactions, affecting the noise exponent; these questions are the focus of ongoing research.

In summary, we find that adsorbed molecular O_2 is a dominant source of magnetism in superconducting devices. The identification of an extrinsic noise source explains the weak dependence of $1/f$ flux noise on device materials and invalidates prevailing theories for the noise based on defects at the metal-insulator interface. Suitable surface passivation and improvements in the sample vacuum environment lead to significant reductions in spin susceptibility and low-frequency flux noise. These developments open the door to the development of frequency-tunable superconducting qubits with improved dephasing times.

We thank M. Aiello, A. Puglielli, and T. Klaus for technical assistance and we acknowledge useful discussions with J. L. DuBois, L. Faoro, L. B. Ioffe, V. Lordi, and J. M. Martinis. This work is supported in part by the U.S. Government under Grants No. W911NF-09-1-0375 and No. W911NF-10-1-0494 and by a gift from Google, Inc. DFT calculations at UCI (H. W. and R. Q. W.) are supported by DOE-BES (Grant No. DE-FG02-05ER46237) and NERSC. Work at Fudan (Z. W. and R. Q. W.) is supported by the CNSF (Grant No. 11474056). Work at the Advanced Photon Source, Argonne is supported by the U.S. Department of Energy, Office of Science under Grant No. DEAC02-06CH11357. NIST acknowledges support from the LPS, ARO, and DARPA.

[1] F. C. Wellstood, C. Urbina, and J. Clarke, Low-frequency noise in dc superconducting quantum interference devices below 1 K, Appl. Phys. Lett. **50**, 772 (1987).

[2] M. B. Weissman, $1/f$ noise and other slow, nonexponential kinetics in condensed matter, Rev. Mod. Phys. **60**, 537 (1988).

[3] F. Yoshihara, K. Harrabi, A. O. Niskanen, Y. Nakamura, and J. S. Tsai, Decoherence of Flux Qubits due to $1/f$ Flux Noise, Phys. Rev. Lett. **97**, 167001 (2006).

[4] K. Kakuyanagi, T. Meno, S. Saito, H. Nakano, K. Semba, H. Takayanagi, F. Deppe, and A. Shnirman, Dephasing of a Superconducting Flux Qubit, Phys. Rev. Lett. **98**, 047004 (2007).

[5] R. C. Bialczak, R. McDermott, M. Ansmann, M. Hofheinz, N. Katz, E. Lucero, M. Neeley, A. D. O'Connell, H. Wang, A. N. Cleland, and J. M. Martinis, $1/f$ Flux Noise in Josephson Phase Qubits, Phys. Rev. Lett. **99**, 187006 (2007).

[6] J. Clarke and F. K. Wilhelm, Superconducting quantum bits, Nature (London) **453**, 1031 (2008).

[7] J. Kelly *et al.*, State preservation by repetitive error detection in a superconducting quantum circuit, Nature (London) **519**, 66 (2015).

[8] A. D. Córcoles, E. Magesan, S. J. Srinivasan, A. W. Cross, M. Steffen, J. M. Gambetta, and J. M. Chow, Demonstration of a quantum error detection code using a square lattice of four superconducting qubits, Nat. Commun. **6**, 6979 (2015).

[9] M. W. Johnson *et al.*, Quantum annealing with manufactured spins, Nature (London) **473**, 194 (2011).

[10] S. Boxio, V. N. Smelyanskiy, A. Shabani, S. V. Isakov, M. Dykman, V. S. Denchev, M. H. Amin, A.Yu. Smirnov, M. Mohseni, and H. Neven, Computational multiqubit tunnelling in programmable quantum annealers, Nat. Commun. **7**, 10327 (2016).

[11] S. Sendelbach, D. Hover, A. Kittel, M. Mück, J. M. Martinis, and R. McDermott, Magnetism in SQUIDs at Millikelvin Temperatures, Phys. Rev. Lett. **100**, 227006 (2008).

[12] L. Faoro and L. B. Ioffe, Microscopic Origin of Low-Frequency Flux Noise in Josephson Circuits, Phys. Rev. Lett. **100**, 227005 (2008).

[13] H. Wang, C. Shi, J. Hu, S. Han, C. C. Yu, and R. Q. Wu, Candidate Source of Flux Noise in SQUIDs: Adsorbed Oxygen Molecules, Phys. Rev. Lett. **115**, 077002 (2015).

[14] S. LaForest and R. de Sousa, Flux-vector model of spin noise in superconducting circuits: Electron versus nuclear spins and role of phase transition, Phys. Rev. B **92**, 054502 (2015).

[15] S. Sendelbach, D. Hover, M. Mück, and R. McDermott, Complex Inductance, Excess Noise, and Surface Magnetism in dc SQUIDs, Phys. Rev. Lett. **103**, 117001 (2009).

[16] S. K. Choi, D.-H. Lee, S. G. Louie, and J. Clarke, Localization of Metal-Induced Gap States at the Metal-Insulator Interface: Origin of Flux Noise in SQUIDs and Superconducting Qubits, Phys. Rev. Lett. **103**, 197001 (2009).

[17] D. Lee, J. L. DuBois, and V. Lordi, Identification of the Local Sources of Paramagnetic Noise in Superconducting Qubit Devices Fabricated on Al_2O_3 Substrates Using Density-Functional Calculations, Phys. Rev. Lett. **112**, 017001 (2014).

[18] See Supplemental Material at http://link.aps.org/supplemental/10.1103/PhysRevApplied.6.041001 for further details.

[19] Yu. A. Freiman and H. J. Jodl, Solid oxygen, Phys. Rep. **401**, 1 (2004).

[20] R. H. Koch, D. P. DiVincenzo, and J. Clarke, Model for $1/f$ Flux Noise in SQUIDs and Qubits, Phys. Rev. Lett. **98**, 267003 (2007).

[21] S. M. Anton, J. S. Birenbaum, S. R. O'Kelley, V. Bolkhovsky, D. A. Braje, G. Fitch, M. Neeley, G. C. Hilton, H.-M. Cho, K. D. Irwin, F. C. Wellstood, W. D. Oliver, A. Shnirman, and J. Clarke, Magnetic Flux Noise in dc SQUIDs: Temperature and Geometry Dependence, Phys. Rev. Lett. **110**, 147002 (2013).

[22] E. Wimmer, H. Krakauer, M. Weinert, and A. Freeman, Full-potential self-consistent linearized-augmented-plane-wave method for calculating the electronic structure of molecules and surfaces: O_2 molecule, Phys. Rev. B **24**, 864 (1981).

[23] J. P. Perdew, K. Burke, and M. Ernzerhof, Generalized Gradient Approximation Made Simple, Phys. Rev. Lett. **77**, 3865 (1996).

[24] R. Q. Wu and A. Freeman, Spin-orbit induced magnetic phenomena in bulk metals and their surfaces and interfaces, J. Magn. Magn. Mater. **200**, 498 (1999).

[25] P. Dutta and P. M. Horn, Low-frequency fluctuations in solids: $1/f$ noise, Rev. Mod. Phys. **53**, 497 (1981).